

## Thickness dependence and dimensionality effects on charge and magnetic orderings in $\text{La}_{1/3}\text{Sr}_{2/3}\text{FeO}_3$ thin films

K. Yamamoto,<sup>1,2,\*</sup> Y. Hirata,<sup>1,2</sup> M. Horio,<sup>2</sup> Y. Yokoyama,<sup>1,2</sup> K. Takubo,<sup>1</sup> M. Minohara,<sup>3</sup> H. Kumigashira,<sup>3</sup> Y. Yamasaki,<sup>4,5,6</sup> H. Nakao,<sup>3</sup> Y. Murakami,<sup>3</sup> A. Fujimori,<sup>2</sup> and H. Wadati<sup>1,2</sup>

<sup>1</sup>*Institute for Solid State Physics, University of Tokyo, Kashiwanoha, Chiba 277-8581, Japan*

<sup>2</sup>*Department of Physics, University of Tokyo, Hongo, Tokyo 113-0033, Japan*

<sup>3</sup>*Institute of Materials Structure Science, High Energy Accelerator Research Organization, Tsukuba, Ibaraki 305-0801, Japan*

<sup>4</sup>*Research and Services Division of Materials Data and Integrated System (MaDIS), National Institute for Materials Science (NIMS), Tsukuba 305-0047, Japan*

<sup>5</sup>*PRESTO, Japan Science and Technology Agency (JST), Kawaguchi 332-0012, Japan*

<sup>6</sup>*RIKEN Center for Emergent Matter Science (CEMS), Wako 351-0198, Japan*



(Received 9 June 2017; revised manuscript received 12 November 2017; published 16 February 2018)

We investigate the thickness effects on charge and magnetic orderings in Fe perovskite oxide  $\text{La}_{1/3}\text{Sr}_{2/3}\text{FeO}_3/\text{SrTiO}_3$  thin films by hard x-ray and resonant soft x-ray scattering (RSXS) with changing thin-film thickness systematically. We found that the correlation lengths of the magnetic ordering along the in-plane and out-of-plane directions are comparable and proportional to the thickness, and show stronger thickness dependence than those of charge ordering. The magnetic ordered states disappear when the correlation length of magnetic ordering decreases to that of charge ordering through the intrinsic thickness effects. Surface-sensitive grazing-incident RSXS revealed that the orderings exist even in the surface region, which indicates that the observed orderings are not affected by surface effects like oxygen vacancies. Critical thickness is in 5–15 nm, which corresponds to 4–11 antiferromagnetic ordering period. This critical value seems to be common to other ferromagnetic oxide thin films.

DOI: [10.1103/PhysRevB.97.075134](https://doi.org/10.1103/PhysRevB.97.075134)

### I. INTRODUCTION

Charge, spin, and orbital orderings in  $3d$  transition-metal perovskite oxides closely relate to the origin of remarkable physics phenomena such as metal-insulator transition, superconductivity, and giant magnetoresistance [1,2]. For instance, stripe structures of spin and charge ordering in superconducting cuprates were reported [3,4] and the charge density wave was found to compete with superconducting states [5–7].

One such  $3d$  transition-metal oxide,  $\text{La}_{1/3}\text{Sr}_{2/3}\text{FeO}_3$ , attracts much attention due to its unusual high valence state and charge disproportionation. Mössbauer spectroscopy showed charge disproportionation of  $3\text{Fe}^{3.67+} \rightarrow 2\text{Fe}^{3+} + \text{Fe}^{5+}$  accompanied by an antiferromagnetic ordering at critical temperature  $T_{\text{CD}} \approx 190\text{K}$  [8,9]. Electronic conductivity shows a transition associated with the charge disproportionation transition at  $T_{\text{CD}}$  [8]. Neutron scattering study revealed that charge and magnetic orderings exist along the [111] direction and Fe layers stack in the sequence of  $\text{Fe}^{3+\uparrow} - \text{Fe}^{5+\uparrow} - \text{Fe}^{3+\uparrow} - \text{Fe}^{3+\downarrow} - \text{Fe}^{5+\downarrow} - \text{Fe}^{3+\downarrow}$  as shown in Fig. 1(a) [10]. Electron diffraction demonstrated structural distortion along the [111] direction [11]. This stacking layer structure is also supported by the exchange interaction determined by inelastic neutron scattering [12] and Hartree-Fock calculation [13]. As for the electronic structure,

x-ray absorption spectroscopy of  $\text{Fe } 2p \rightarrow 3d$  and  $\text{O } 1s \rightarrow 2p$  suggests that holes induced by Sr doping exhibits O  $2p$  hole character [14]. The unusually high valence states  $\text{Fe}^{4+}$  and  $\text{Fe}^{5+}$  are expressed rather as  $3d^5\bar{L}$  and  $3d^5\bar{L}^2$ , where  $\bar{L}$  represents an O  $2p$  hole [1,14,15].

The electronic states of thin films are sometimes different from those of the bulk. Especially, the thinnest limit of the ordered states, critical thickness, is an important parameter to understand the dimensionality effects. We focused on the relationship of critical thickness and ordered structure for antiferromagnetic  $\text{La}_{1/3}\text{Sr}_{2/3}\text{FeO}_3$ . The charge ordering exists even in  $\text{La}_{1/3}\text{Sr}_{2/3}\text{FeO}_3$  thin films [16–20]. This is considered to be due to the small lattice distortion accompanied by the charge disproportionation in contrast to the case of  $\text{Fe}^{4+}$  oxide  $\text{CaFeO}_3$  [21] or Mn perovskite oxides such as  $\text{Pr}_{1-x}\text{Ca}_x\text{MnO}_3$  and  $\text{Nd}_{1-x}\text{Sr}_x\text{MnO}_3$  [22]. For this reason,  $\text{La}_{1/3}\text{Sr}_{2/3}\text{FeO}_3$  thin film is a suitable material for extracting intrinsic effects of thickness and dimensionality on electronic states without the influence of lattice distortion. However, there have been no studies of thickness effect except for resistivity measurements [23,24]. Minohara *et al.* studied the precise thickness dependence of resistivity in  $\text{La}_{1/3}\text{Sr}_{2/3}\text{FeO}_3/\text{SrTiO}_3$  thin films and found that the ordered states were suppressed with thickness  $t$  below 14 nm as shown by  $\rho - T$  curves in Fig. 1(b) [23]. Resistivity becomes too high to determine the resistivity jump with decreasing thickness due to the insulating  $\text{SrTiO}_3$  substrates and resistivity is not a direct evidence for the orderings. Therefore, x-ray is the most suitable experimental technique for directly observing ordered

\*<http://sites.google.com/site/yamakolux>; [yamako@issp.u-tokyo.ac.jp](mailto:yamako@issp.u-tokyo.ac.jp)

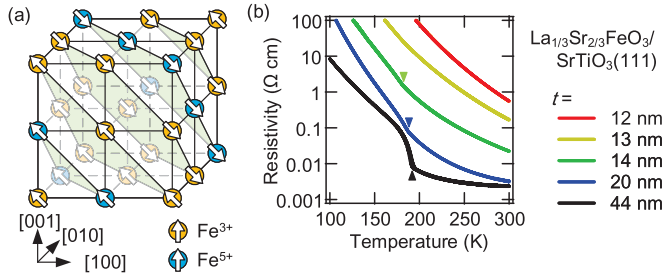


FIG. 1. Charge disproportionation in  $\text{La}_{1/3}\text{Sr}_{2/3}\text{FeO}_3$ . (a) Schematic drawing of charge and spin ordered structure of  $\text{La}_{1/3}\text{Sr}_{2/3}\text{FeO}_3$  determined by neutron [10] and electron diffraction [11]. (b) Temperature dependence of electric resistivity of  $\text{La}_{1/3}\text{Sr}_{2/3}\text{FeO}_3/\text{SrTiO}_3$  thin films reproduced from Minohara *et al.* [23].

states of superstructure peaks and for determining the critical thickness.

Okamoto *et al.* performed hard x-ray scattering for charge ordering and resonant soft x-ray scattering (RSXS) for magnetic ordering at the  $\text{Fe } 2p_{3/2} \rightarrow 3d$  absorption [17]. They evaluated correlation lengths especially around  $T_{\text{CD}}$  and discussed the magnetic ordered states. Correlation length is a physical quantity which characterizes ordered states, and we evaluated correlation lengths of both charge and magnetic ordering with thin films of various thickness in wide range of temperature including well below  $T_{\text{CD}}$ . One cannot observe the magnetic ordering peak ( $\frac{1}{6} \frac{1}{6} \frac{1}{6}$ ) by hard x-ray [17] due to the small cross section of magnetic scattering [25]. RSXS is a suitable technique to study magnetic orderings in thin films and small crystals [5–7, 17, 25–31]. We obtained a strong sensitivity of magnetic scattering at the  $\text{Fe } 2p \rightarrow 3d$  absorption edge due to strong spin-orbit coupling of  $\text{Fe } 2p$  core levels. We measured correlation lengths of charge orderings by hard x-ray scattering and magnetic ordering by RSXS, respectively, with varying thickness systematically. In addition to reflection geometry RSXS, we performed grazing-incident RSXS (GI-RSXS). When the incident angle is below the total reflection angle, the probing depth of x-ray becomes small and one can access surface-sensitive information. This technique was used to study surface states of ordering and revealed that surface melting in  $\text{La}_{0.5}\text{Sr}_{1.5}\text{MnO}_4$  [32,33] and surface orbital ordering in  $\text{LaCoO}_3$  thin films [31].

## II. EXPERIMENT

The  $\text{La}_{1/3}\text{Sr}_{2/3}\text{FeO}_3$  thin films were grown on  $\text{SrTiO}_3(111)$  and (110) substrates by pulsed laser deposition method. The details of the sample fabrication were described elsewhere [23]. The thickness of the thin films was determined from the Laue fringes around the (111) Bragg peaks (not shown). We performed hard x-ray scattering experiments for  $\text{La}_{1/3}\text{Sr}_{2/3}\text{FeO}_3$  ( $t = 5, 15, 17,$  and  $78 \text{ nm}$ )/ $\text{SrTiO}_3(111)$  thin films at BL-4C of Photon Factory, KEK. We measured the charge ordering peak ( $\frac{4}{3} \frac{4}{3} \frac{4}{3}$ ) with hard x-ray. The experimental geometry is shown in Fig. 2(a). The incident photon energy of x-ray was 12.4 keV. Incident x-ray was  $\sigma$ -polarized and scattered x-ray was detected without polarization analysis and hence includes  $\sigma'$ - and  $\pi'$ -polarized photons. We performed RSXS experiments

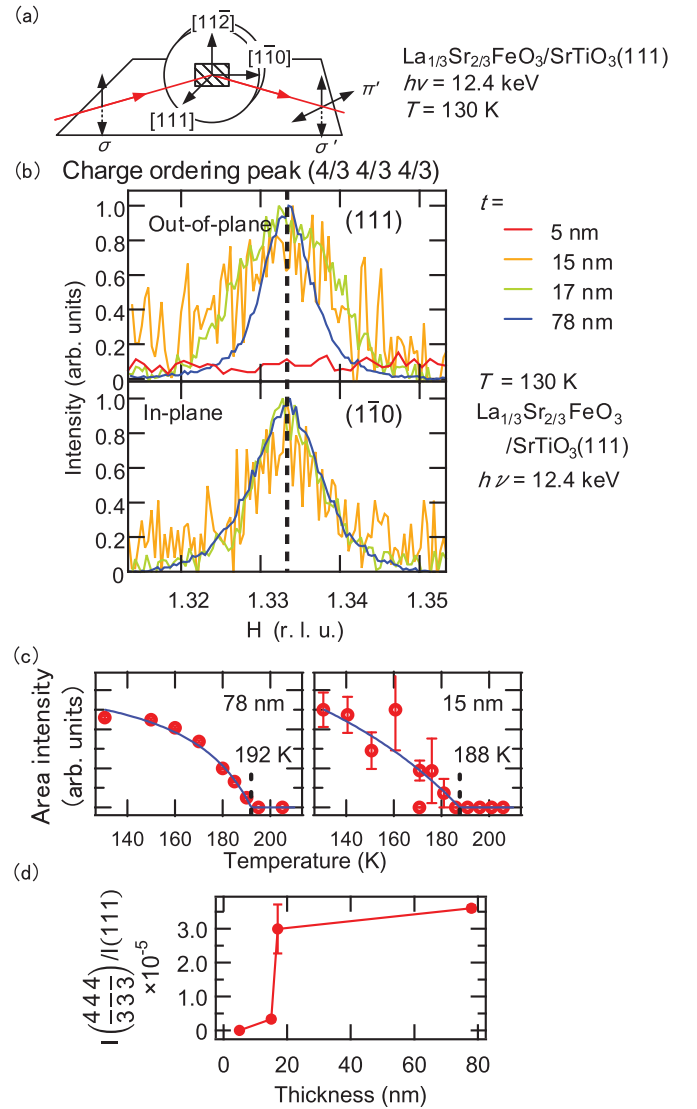


FIG. 2. Observation of charge ordering by hard x-ray diffraction. (a) Experimental setup.  $\pi$ ,  $\pi'$ , and  $\sigma'$  indicate the directions of polarizations of x-rays. (b) Charge ordering peaks ( $\frac{4}{3} \frac{4}{3} \frac{4}{3}$ ) observed along the out-of-plane and in-plane directions at 130 K. (c) Temperature dependence of area intensity of the charge ordering peak. The lines are guides to the eye. (d) Charge ordering peak intensity normalized by the lattice Bragg peak (111) intensity plotted as a function of thickness.

for  $\text{La}_{1/3}\text{Sr}_{2/3}\text{FeO}_3$  ( $t = 5, 17, 37,$  and  $78 \text{ nm}$ )/ $\text{SrTiO}_3(111)$  thin films at the BL-19B of Photon Factory. We observed the magnetic ordering scattering peak ( $\frac{1}{6} \frac{1}{6} \frac{1}{6}$ ) by RSXS. The incident photon energy was 707 eV at the  $\text{Fe } 2p_{3/2} \rightarrow 3d$  absorption edge. Incident x-ray was  $\pi$ -polarized and scattered photon was detected by an energy-resolved silicon drift detector without polarization analysis. We removed O  $K_{\alpha}$  fluorescence emission by tuning energy windows to the Fe L edge. The geometry is shown in Fig. 3(a). The sample was  $\text{La}_{1/3}\text{Sr}_{2/3}\text{FeO}_3(40 \text{ nm})/\text{SrTiO}_3(110)$ , which has in-plane modulation vectors. To investigate the surface states, we performed GI-RSXS in the geometry shown in Fig. 4(a) using the sample  $\text{La}_{1/3}\text{Sr}_{2/3}\text{FeO}_3(40 \text{ nm})/\text{SrTiO}_3(110)$ , which has in-plane modulation vectors.

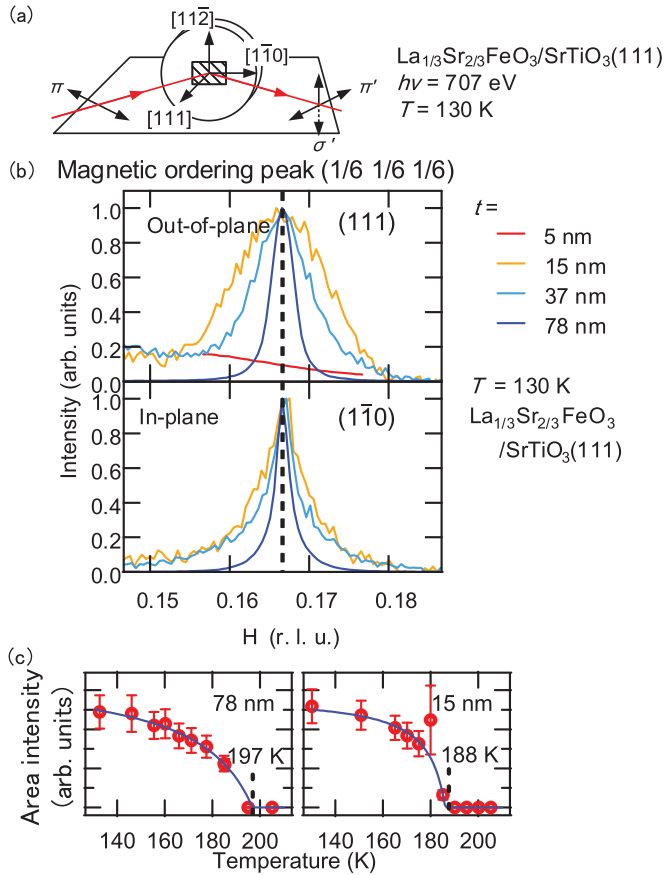


FIG. 3. Observation of magnetic ordering by RSXS. (a) Experimental setup.  $\pi$ ,  $\pi'$ , and  $\sigma'$  indicate the directions of polarizations of x-rays. (b) Magnetic ordering peaks ( $\frac{1}{6}\frac{1}{6}\frac{1}{6}$ ) observed along the out-of-plane and in-plane directions at 130 K. (c) Temperature dependence of area intensity of the magnetic ordering peak. The lines are guides to the eye.

### III. RESULTS AND DISCUSSION

Figure 2(b) shows the charge ordering peak ( $\frac{4}{3}\frac{4}{3}\frac{4}{3}$ ) along the out-of-plane [111] direction and along the in-plane  $[1\bar{1}0]$  direction. The charge orderings exist in  $t = 15$  nm, and disappears in  $t = 5$  nm. The peak width shows little dependence on thickness. Figure 2(c) shows the temperature dependence of the peak intensity. The critical temperature  $T_{CD}$  was determined from this dependence. Figure 2(d) shows that the charge ordering peak intensity drops sharply when the thickness is reduced to 15 nm. This drop suggests that critical thickness  $t_c$  exists and the value is  $t_c \sim 10$  nm, which is in good agreement with the previous electric resistivity study [23]. Figure 3(b) shows the magnetic ordering peak ( $\frac{1}{6}\frac{1}{6}\frac{1}{6}$ ) along both directions. The peak width increases when thickness becomes thinner and the peak disappears at  $t = 5$  nm. This disappearance is also consistent with the charge ordering behavior shown in Figs. 2(b) and 2(d). The correlation length is given as the reciprocal of the full width at the half maximum, namely,  $2\pi/\Delta q$ , which is the same definition as previous reports [19,30,34]. This peak width tendency of the magnetic ordering indicates that correlation length decreases when thickness becomes thinner. The critical temperature was also determined

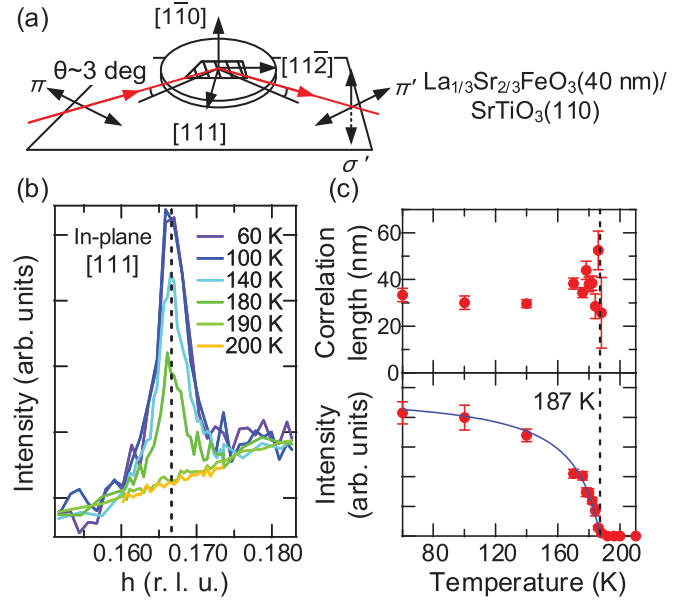


FIG. 4. Observation of the magnetic ordering peak by GI-RSXS. (a) Experimental setup.  $\pi$ ,  $\pi'$ , and  $\sigma'$  indicate the directions of polarizations of x-rays. (b) Magnetic ordering peaks ( $\frac{1}{6}\frac{1}{6}\frac{1}{6}$ ). (c) Correlation length and peak area intensity plotted as a function of temperature.

by the temperature dependence of the peak intensity as shown in Fig. 3(c). The correlation length and the critical temperature of the charge and magnetic ordered states are summarized in Fig. 5 and will be discussed later.

It may be the case that surface states differ from bulk states by possible oxygen vacancies due to the high valence state of  $\text{Fe}^{3.67+}$ . Effects of oxygen vacancy affects the orderings [19,20] and probing surface state is important for studying the thickness dependence. We performed GI-RSXS study to investigate the surface states. We studied  $\text{La}_{1/3}\text{Sr}_{2/3}\text{FeO}_3(40\text{ nm})/\text{SrTiO}_3(110)$  thin films with the in-plane modulation vector and measured the magnetic orderings peak ( $\frac{1}{6}\frac{1}{6}\frac{1}{6}$ ). Its probing depth was determined to be approximately 2 nm by calculation from x-ray absorption spectroscopy and the incident angle. Figure 4(b) shows the result of GI-RSXS and Fig. 4(c) shows the correlation length and the transition temperature.  $T_{CD}$  and the peak position of surface states are the same as those of bulk states shown in Fig. 5 and correlation length is in the same order of the results of the bulk state. These results indicate that the surface states of  $\text{La}_{1/3}\text{Sr}_{2/3}\text{FeO}_3$  thin films are the same as the bulk state and the measured thickness dependence is not due to the surface effects but due to intrinsic dimensionality effects. These results are also consistent with small dependence on thin film coordinates measured by electronic resistivity study [23]. We remark that scattering peak width along the out-of-plane direction is broadened due to the limited probing depth and only the in-plane GI-RSXS measurement results are shown. As for the interfaces between sample and substrate, Minohara *et al.* showed the chemically abrupt interfaces from the results of electron microscopy image along the out-of-plane direction in the same type of system [23].

The obtained correlation length is plotted as a function of thickness in Fig. 5(a) at 130 K. The experimental resolution

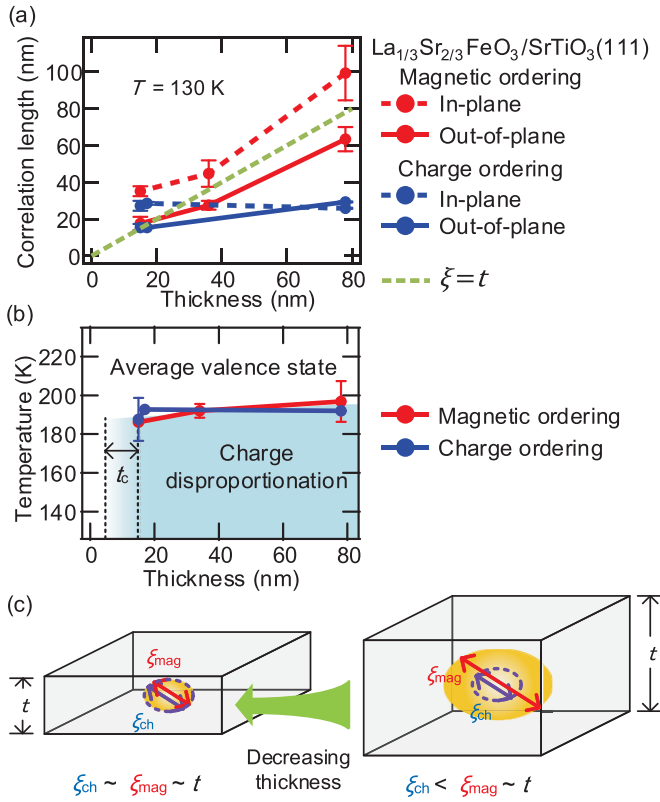


FIG. 5. Thickness dependence in  $\text{La}_{1/3}\text{Sr}_{2/3}\text{FeO}_3$  thin films revealed by x-ray scattering. (a) Correlation length of magnetic and charge ordering for various thickness thin films. These values were determined by hard and soft x-ray scattering results. Dotted line  $\xi = t$  is also plotted. (b) Phase diagrams estimated from the temperature dependence of charge and magnetic ordering peak intensities in  $\text{La}_{1/3}\text{Sr}_{2/3}\text{FeO}_3/\text{SrTiO}_3(111)$  thin films.  $t_c$  indicates the critical thickness of the charge disproportionation. (c) Schematic illustration of the thickness dependent change of ordered states.

is presented in the Appendix. Both out-of-plane and in-plane correlation lengths of magnetic orderings matches thickness, as shown by the line  $\xi = t$  in Fig. 5(a). Geometrical limitation of thickness explains this behavior of the out-of-plane correlation length. However, the in-plane correlation length also decreases when the thickness of the thin film becomes thinner. This behavior suggests that magnetic orderings have an isotropic correlation. Comparing with correlation length of magnetic ordering  $\xi_{\text{mag}} = 2\pi/\Delta q(\frac{1}{6} \frac{1}{6} \frac{1}{6})$ , the thickness dependence of the correlation length of charge orderings  $\xi_{\text{ch}} = 2\pi/\Delta q(\frac{4}{3} \frac{4}{3} \frac{4}{3})$  is much weaker than that of magnetic orderings. When the thickness is sufficiently large ( $\sim 78 \text{ nm}$ ), the correlation length of magnetic ordering is in the same order of thickness ( $\xi_{\text{ch}} < \xi_{\text{mag}} \sim t$ ). When the thickness and  $\xi_{\text{mag}}$  reach  $\xi_{\text{ch}}$  at the thickness of approximately 15 nm ( $\xi_{\text{ch}} \sim \xi_{\text{mag}} \sim t$ ), the orderings disappear. This indicates that a minimal value of domain size of  $\sim 15 \text{ nm}$  exists, and thickness limitation makes the correlation length of magnetic ordering below the minimal value and suppresses the orderings. We obtained the critical temperature  $T_{\text{CD}}$  from temperature dependence of scattering peak area intensity and it is plotted as a function of thickness as shown in Fig. 5(b).  $T_{\text{CD}}$  slightly decreased when thin films became thinner, and  $T_{\text{CD}}$  of charge and magnetic orderings

were almost the same. This slight decrease is consistent with other magnetic ordered compounds and matches the result of resistivity study [23]. These behaviors are schematically shown in Fig. 5(c). The mechanism which explains why  $\xi_{\text{mag}}$  is longer than  $\xi_{\text{ch}}$  is uncertain. It may be related to the previous results of neutron scattering experiment [12], which suggests the charge ordering is stabilized by magnetic ordering. The obtained critical thickness of 5–15 nm corresponds to 4–11 units with the antiferromagnetic ordering period of 6 u.c. as a unit. This critical number of units seems to be common to other ferromagnetic perovskite oxide  $\text{La}_{1-x}\text{Sr}_x\text{MnO}_3$  ( $x = 0.3\text{--}0.4$ ) (3–8 units [35,36]).

#### IV. CONCLUSION

In summary, we performed hard x-ray scattering and RSXS experiments for the charge and magnetic orderings in  $\text{La}_{1/3}\text{Sr}_{2/3}\text{FeO}_3/\text{SrTiO}_3$  thin films with changing the thickness systematically. We also performed GI-RSXS experiments to investigate surface states of  $\text{La}_{1/3}\text{Sr}_{2/3}\text{FeO}_3$  thin films with the unusually high valence state. Magnetic ordering is stable even in the surface region in spite of its high valence states, and this suggests that the thickness dependence comes from the intrinsic geometrical effects. The correlation length of the magnetic ordering  $\xi_{\text{mag}}$  is comparable and proportional to the thickness. Reduced thickness suppresses the ordered states at the critical temperature  $t_c$  through this relationship between  $t$  and  $\xi_{\text{mag}}$ . It will be interesting to study, systematically, thickness dependences of charge, magnetic, or orbital orderings with x-ray scattering for various thin films and elucidate behaviors especially around critical thicknesses.

#### ACKNOWLEDGMENTS

X-ray scattering measurements were performed under the approval of the Photon Factory Program Advisory Committee (Proposals No. 2015G556, No. 2016PF-BL-19B, No. 2015S2-007) at the Institute of Material Structure Science, High Energy Accelerator Research Organization (KEK). This article was partially supported by the Ministry of Education, Culture,

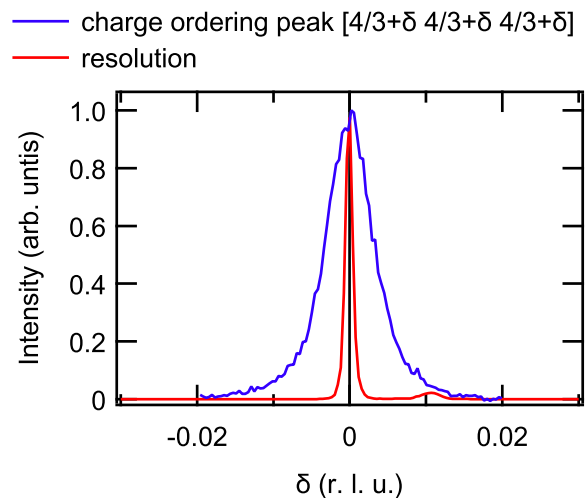


FIG. 6. Diffraction peak and resolution. The nonmagnetic diffraction data  $q = [111]$  of  $\text{SrTiO}_3$  substrate is shown as resolution.

Sports, Science and Technology (MEXT), Japan (X-ray Free Electron Laser Priority Strategy Program). This work was financially supported by Grants-in-Aid for Scientific Research (Grants No. 16H02115, No. 16H05990, No. 16K17722) from the Japan Society for the Promotion of Science (JSPS). This research was supported in part by PRESTO Grant No. JPMJPR177A from Japan Science and Technology Agency (JST), “Materials research by Information Integration” Initiative (MI2I) project of the Support Program for Starting Up Innovation Hub from JST and JSPS through the Funding Program for World-Leading Innovative R&D on Science and Technology (FIRST Program). K. Y. acknowledges the support from the ALPS program of the University of Tokyo and from the Motizuki Fund of Yukawa Memorial Foundation.

## APPENDIX: COMPARISON OF RESOLUTION AND DIFFRACTION PEAK

In this appendix, we show that resolution of this diffraction experiment has small effects on the discussion and conclusion. We evaluated the resolution of hard x-ray diffraction with assuming that the structural diffraction peak of the substrate is sufficiently sharp and the width of this peak mainly reflects the instrumental resolution. Figure 6 shows the charge ordering peak and structural diffraction peak of substrate, which is equivalent to the resolution. The resolution is  $0.033\text{nm}^{-1}$  and this value is approximately 6 times higher than the super lattice peak. As for the soft x-ray diffraction, wavelength is approximately 10 times longer than that of hard x-ray and therefore the resolution has a smaller effect than the hard x-ray case.

- 
- [1] M. Imada, A. Fujimori, and Y. Tokura, *Rev. Mod. Phys.* **70**, 1039 (1998).
- [2] Y. Tokura and N. Nagaosa, *Science* **288**, 462 (2000).
- [3] J. M. Tranquada, B. J. Sternlieb, J. D. Axe, Y. Nakamura, and S. Uchida, *Nature* **375**, 561 (1995).
- [4] J. M. Tranquada, *J. Phys. Chem. Solids* **59**, 2150 (1998).
- [5] G. Ghiringhelli, M. Le Tacon, M. Minola, S. Blanco-Canosa, C. Mazzoli, N. B. Brookes, G. M. De Luca, A. Frano, D. G. Hawthorn, F. He, T. Loew, M. M. Sala, D. C. Peets, M. Salluzzo, E. Schierle, R. Sutarto, G. A. Sawatzky, E. Weschke, B. Keimer, and L. Braicovich, *Science* **337**, 821 (2012).
- [6] S. Blanco-Canosa, A. Frano, T. Loew, Y. Lu, J. Porras, G. Ghiringhelli, M. Minola, C. Mazzoli, L. Braicovich, E. Schierle, E. Weschke, M. Le Tacon, and B. Keimer, *Phys. Rev. Lett.* **110**, 187001 (2013).
- [7] J. He, P. Shafer, T. R. Mion, V. T. Tra, Q. He, J. Kong, Y.-D. Chuang, W. L. Yang, M. J. Graf, J.-Y. Lin, Y.-H. Chu, E. Arenholz, and R.-H. He, *Nat. Commun.* **7**, 10852 (2016).
- [8] M. Takano and Y. Takeda, *Bull. Inst. Chem. Res. Kyoto Univ.* **61**, 406 (1983).
- [9] P. Battle, T. Gibb, and S. Nixon, *J. Solid State Chem.* **77**, 124 (1988).
- [10] P. Battle, T. Gibb, and P. Lightfoot, *J. Solid State Chem.* **84**, 271 (1990).
- [11] J. Q. Li, Y. Matsui, S. K. Park, and Y. Tokura, *Phys. Rev. Lett.* **79**, 297 (1997).
- [12] R. J. McQueeney, J. Ma, S. Chang, J.-Q. Yan, M. Hehlen, and F. Trouw, *Phys. Rev. Lett.* **98**, 126402 (2007).
- [13] T. Mizokawa and A. Fujimori, *Phys. Rev. Lett.* **80**, 1320 (1998).
- [14] M. Abbate, F. M. F. de Groot, J. C. Fuggle, A. Fujimori, O. Strelbel, F. Lopez, M. Domke, G. Kaindl, G. A. Sawatzky, M. Takano, Y. Takeda, H. Eisaki, and S. Uchida, *Phys. Rev. B* **46**, 4511 (1992).
- [15] A. E. Bocquet, T. Mizokawa, T. Saitoh, H. Namatame, and A. Fujimori, *Phys. Rev. B* **46**, 3771 (1992).
- [16] H. Wadati, D. Kobayashi, H. Kumigashira, K. Okazaki, T. Mizokawa, A. Fujimori, K. Horiba, M. Oshima, N. Hamada, M. Lippmaa, M. Kawasaki, and H. Koinuma, *Phys. Rev. B* **71**, 035108 (2005).
- [17] J. Okamoto, D. J. Huang, K. S. Chao, S. W. Huang, C.-H. Hsu, A. Fujimori, A. Masuno, T. Terashima, M. Takano, and C. T. Chen, *Phys. Rev. B* **82**, 132402 (2010).
- [18] K. Ueno, A. Ohtomo, F. Sato, and M. Kawasaki, *Phys. Rev. B* **73**, 165103 (2006).
- [19] R. J. Sichel-Tissot, R. C. Devlin, P. J. Ryan, J.-W. Kim, and S. J. May, *Appl. Phys. Lett.* **103**, 212905 (2013).
- [20] Y. Xie, M. D. Scafetta, R. J. Sichel-Tissot, E. J. Moon, R. C. Devlin, H. Wu, A. L. Krick, and S. J. May, *Adv. Mater.* **26**, 1434 (2014).
- [21] J. Matsuno, M. Seto, S. Kitao, Y. Kobayashi, R. Haruki, T. Mitsui, A. Fujimori, Y. Takeda, S. Kawasaki, and M. Takano, *J. Phys. Soc. Jpn.* **73**, 2768 (2004).
- [22] Y. Tokura, *Rep. Prog. Phys.* **69**, 797 (2006).
- [23] M. Minohara, M. Kitamura, H. Wadati, H. Nakao, R. Kumai, Y. Murakami, and H. Kumigashira, *J. Appl. Phys.* **120**, 025303 (2016).
- [24] R. C. Devlin, A. L. Krick, R. J. Sichel-Tissot, Y. J. Xie, and S. J. May, *J. Appl. Phys.* **115**, 233704 (2014).
- [25] M. Blume, *J. Appl. Phys.* **57**, 3615 (1985).
- [26] J. Fink, E. Schierle, E. Weschke, and J. Geck, *Rep. Prog. Phys.* **76**, 056502 (2013).
- [27] T. Matsuda, S. Partzsch, T. Tsuyama, E. Schierle, E. Weschke, J. Geck, T. Saito, S. Ishiwata, Y. Tokura, and H. Wadati, *Phys. Rev. Lett.* **114**, 236403 (2015).
- [28] H. Wadati, J. Okamoto, M. Garganourakis, V. Scagnoli, U. Staub, Y. Yamasaki, H. Nakao, Y. Murakami, M. Mochizuki, M. Nakamura, M. Kawasaki, and Y. Tokura, *Phys. Rev. Lett.* **108**, 047203 (2012).
- [29] D. J. Huang, H.-J. Lin, J. Okamoto, K. S. Chao, H.-T. Jeng, G. Y. Guo, C.-H. Hsu, C.-M. Huang, D. C. Ling, W. B. Wu, C. S. Yang, and C. T. Chen, *Phys. Rev. Lett.* **96**, 096401 (2006).
- [30] H. Wadati, J. Geck, E. Schierle, R. Sutarto, F. He, D. G. Hawthorn, M. Nakamura, M. Kawasaki, Y. Tokura, and G. A. Sawatzky, *New J. Phys.* **16**, 033006 (2014).
- [31] Y. Yamasaki, J. Fujioka, H. Nakao, J. Okamoto, T. Sudayama, Y. Murakami, M. Nakamura, M. Kawasaki, T. Arima, and Y. Tokura, *J. Phys. Soc. Jpn.* **85**, 023704 (2016).
- [32] Y. Wakabayashi, M. H. Upton, S. Grenier, J. P. Hill, C. S. Nelson, J.-W. Kim, P. J. Ryan, A. I. Goldman, H. Zheng, and J. F. Mitchell, *Nat. Mater.* **6**, 972 (2007).
- [33] S. B. Wilkins, X. Liu, Y. Wakabayashi, J.-W. Kim, P. J. Ryan, H. Zheng, J. F. Mitchell, and J. P. Hill, *Phys. Rev. B* **84**, 165103 (2011).

- [34] S. Y. Zhou, Y. Zhu, M. C. Langner, Y.-D. Chuang, P. Yu, W. L. Yang, A. G. Cruz Gonzalez, N. Tahir, M. Rini, Y.-H. Chu, R. Ramesh, D.-H. Lee, Y. Tomioka, Y. Tokura, Z. Hussain, and R. W. Schoenlein, *Phys. Rev. Lett.* **106**, 186404 (2011).
- [35] M. Huijben, L. W. Martin, Y.-H. Chu, M. B. Holcomb, P. Yu, G. Rijnders, D. H. A. Blank, and R. Ramesh, *Phys. Rev. B* **78**, 094413 (2008).
- [36] K. Yoshimatsu, K. Horiba, H. Kumigashira, E. Ikenaga, and M. Oshima, *Appl. Phys. Lett.* **94**, 071901 (2009).